A Fast Noise and Z-Parameter Transformations Between Common Emitter and Common Base InP DHBT

Yong Zhong Xiong, *Member, IEEE*, Geok-Ing Ng, *Senior Member, IEEE*, Hong Wang, *Member, IEEE*, Chee Leong Tan, *Student Member, IEEE*, and J. S. Fu, *Senior Member, IEEE*

***Abstract*—A new approach has been developed that uses only a simple set of formulas to transform noise and Z- parameters between common emitter and common base configurations. This technique is based on the typical T-model of InP double-heterojunction bipolar transistor and calculated results agree with the experimental results, demonstrating that this approach is useful for many broad-band low-noise communication circuit designs.**

***Index Terms*—Common base, common emitter, InP HBT, noise figure, noise parameters, Z-parameters.**

I. Introduction

As IS commonly known, the noise performance for a common emitter (CE) and the common base (CB) configuration at very low frequencies is identical [1], [2]. However, there are some differences at RF and microwave frequency band due to the base–collector (BC) feedback capacitance of the CE configuration. A circuit configuration in the CE mode usually produces more noise than its CB counterpart. This is primarily due to its high input impedance that makes broad-band matching more difficult. A CB configuration has the advantages of ease of broad-band impedance matching, at better gain and a lower noise figure [3], [4]. Therefore, a CB configuration is generally more suitable for optical and microwave broad-band communication applications. However, current methods to calculate the CB noise parameters using available CE noise parameters are usually complicated and time consuming [5], [6]. In this paper, we propose a simple, yet effective transformation technique to convert the CE noise parameters into the CB noise parameters. Also, the transformations of the Z-parameters between the CE and CB configurations are presented. In this paper, an InP-based double-heterojunction bipolar transistor (DHBT) is used to illustrate this method.

II. Model

A. Z-Parameter Transformation Between CE and CB

A typical T-model is used for the InP DHBT and its equivalent circuit in the CE configuration is shown in Fig. 1 [7]. The

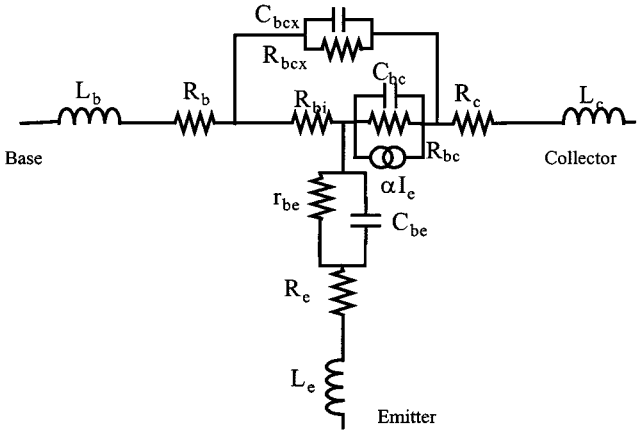

Fig. 1. T-model in CE configuration.

Z-parameter expressions for the small-signal equivalent circuit of heterojunction bipolar transistors (HBTs) are derived in [8]. The extrinsic capacitances to ground are small for the devices using on-wafer probing. They are not suspected to significantly influence the results based on the analysis presented. Its corresponding small-signal equivalent circuit in the CB configuration can be obtained from rotating Fig. 1 by 90°. The Z-parameter expressions for the CB configuration are

$$Z_{11}^{\mathrm{CB}} = z_E + z_B + \frac{(1-\alpha)z_{\mathrm{BC}}R_{bi} + z_F R_{bi}}{\Delta} \tag{1}$$

$$Z_{12}^{\mathrm{CB}} = z_B + \frac{z_F R_{bi}}{\Delta} \tag{2}$$

$$Z_{21}^{\mathrm{CB}} = z_B + \frac{\alpha z_{\mathrm{BC}} z_F + z_F R_{bi}}{\Delta} \tag{3}$$

$$Z_{zz}^{\mathrm{CB}} = z_C + z_B + \frac{(z_{\mathrm{BC}} + R_{bi})z_F}{\Delta} \tag{4}$$

where $\Delta = Z_{\mathrm{BC}} + Z_F + R_{bi}$ and Z_{ij}^{CB} denotes CB Z-parameters.

Comparing the Z-parameters of the CE and the CB configurations, we can get the following relations:

$$Z_{11}^{\mathrm{CB}} = Z_{11}^{\mathrm{CE}} \tag{5}$$

$$Z_{12}^{\mathrm{CB}} = Z_{11}^{\mathrm{CE}} - Z_{12}^{\mathrm{CE}} \tag{6}$$

$$Z_{21}^{\mathrm{CB}} = Z_{11}^{\mathrm{CE}} - Z_{21}^{\mathrm{CE}} \tag{7}$$

$$Z_{22}^{\mathrm{CB}} = Z_{11}^{\mathrm{CE}} + Z_{22}^{\mathrm{CE}} - Z_{12}^{\mathrm{CE}} - Z_{21}^{\mathrm{CE}} \tag{8}$$

Manuscript received December 3, 2000. This work was supported by the National Science and Technology Board of Singapore (EMT/99/011).

Y. Z. Xiong, G.-I. Ng, H. Wang, and J. S. Fu are with the Microelectronics Center, School of Electrical and Electronics Engineering, Nanyang Technological University, Singapore 639798, Singapore (e-mail: yongzhong@ime.org.sg).

C. L. Tan is with the Defence Science Organization National Laboratories, Singapore 118230, Singapore.

Publisher Item Identifier S 0018-9480(02)03014-4.

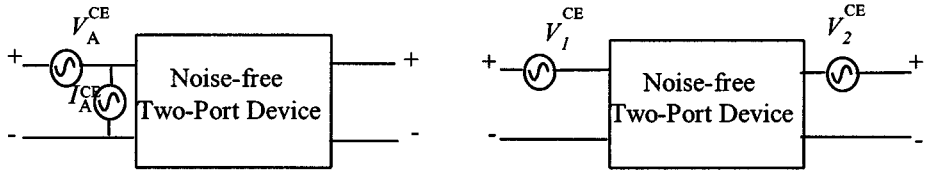

Fig. 2. (a) Two-port device of a CE HBT with its noise represented by equivalent input sources: one current gerentor and one voltage gerentor. (b) Two-port device of a CE HBT with its noise represented by equivalent input sources: two voltage gerentors.

and the $ABCD$-parameter transformations

$$A^{\rm CB} = \frac{A^{\rm CE}}{A^{\rm CE}-1} \tag{9}$$

$$C^{\rm CB} = \frac{C^{\rm CE}}{A^{\rm CE}-1} \tag{10}$$

where $Z_{ij}^{\rm CE}$ denotes the CE Z-parameters, and $A^{\rm CB}$, $C^{\rm CB}$ and $A^{\rm CE}$, $C^{\rm CE}$ denote the $ABCD$-parameters of the CB and CE configurations, respectively.

B. Noise Parameter Transformation Between CE and CB

Fig. 2(a) shows the two-port device of a CE HBT with its noise represented by an equivalent input source: a current generator and a voltage generator. These sources and their correlation coefficient completely characterize the noise of the device. Normally these sources are specified by the following standard set of noise parameters [9]:

$$R_n^{\rm CE} = \frac{\langle \bar{v}_A^2 \rangle}{4kT_0} \tag{11}$$

$$G_n^{\rm CE} = \frac{\langle \bar{i}_A^2 \rangle}{4kT_0} \tag{12}$$

$$Y_{\rm cor}^{\rm CE} = G_{\rm cor}^{\rm CE} + jB_{\rm cor}^{\rm CE} = \frac{\langle i_A v_A^* \rangle}{\langle \bar{v}_A^2 \rangle}. \tag{13}$$

These parameters are known as the noise resistance, noise conductance, and correlation admittance, respectively. The Boltzmann's constant and reference temperature are denoted by k and T_0, respectively. The noise sources are defined in terms of spectral densities, i.e., volts and amperes per root hertz. In terms of these parameters, the noise figure of the device is given by [9]

$$F^{\rm CE} = F_{\rm MIN}^{\rm CE} + \frac{R_n^{\rm CE}}{G_s}\left| Y_s - \left(G_{\rm opt}^{\rm CE} + jB_{\rm opt}^{\rm CE}\right)\right|^2 \tag{14}$$

where $Y_s = G_s + jB_s$ is the admittance of the source, and

$$G_{\rm opt}^{\rm CE^2} = G_{\rm cor}^{\rm CE^2} + \frac{G_n^{\rm CE}}{R_n^{\rm CE}} \tag{15}$$

$$B_{\rm opt}^{\rm CE} = -B_{\rm cor}^{\rm CE} \tag{16}$$

and

$$F_{\rm MIN}^{\rm CE} = 1 + 2R_n^{\rm CE}\left(G_{\rm opt}^{\rm CE} + G_{\rm cor}^{\rm CE}\right). \tag{17}$$

Fig. 2(a) shows that the voltage and current noise sources $V_A^{\rm CE}$ and $I_A^{\rm CE}$, the $ABCD$-matrix description, will be more convenient for this linear two-port noise network. This representation is as follows:

$$V_1 = AV_2 + BI_2 + V_A^{\rm CE} \tag{18}$$

$$I_1 = CV_2 + DI_2 + I_A^{\rm CE}. \tag{19}$$

Fig. 2(b) shows the two noise voltage sources at the input and output of the linear two-port noise network; it is relatively easy to derive the expressions in the impedance form as follows:

$$V_1 = Z_{11}I_1 + Z_{12}I_2 + V_1^{\rm CE} \tag{20}$$

$$V_2 = Z_{21}I_1 + Z_{22}V_1 + V_2^{\rm CE}. \tag{21}$$

Comparing (17) and (18) with (19) and (20), we can obtain (22) and (23) as follows:

$$V_1^{\rm CE} = V_A^{\rm CE} - \frac{A^{\rm CE}}{C^{\rm CE}} I_A^{\rm CE} \tag{22}$$

$$V_2^{\rm CE} = -\frac{I_A^{\rm CE}}{C^{\rm CE}} \tag{23}$$

where $A^{\rm CE}$ and $C^{\rm CE}$ denote the $ABCD$-parameters of the two-port device of a CE HBT. Using the method of [5], the CB noise voltage sources $V_1^{\rm CB}$ and $V_2^{\rm CB}$ are derived as

$$V_1^{\rm CB} = -V_1^{\rm CE} \tag{24}$$

$$V_2^{\rm CB} = V_2^{\rm CE} - V_1^{\rm CE} \tag{25}$$

and the voltage and current noise sources $V_A^{\rm CB}$ and $V_A^{\rm CB}$ for the CB configuration are similarly obtained as

$$V_A^{\rm CB} = V_1^{\rm CB} - A^{\rm CB}V_2^{\rm CB} = \frac{V_A^{\rm CE}}{A^{\rm CE}-1} \tag{26}$$

$$I_A^{\rm CB} = -C^{\rm CB}V_2^{\rm CB} = \frac{C^{\rm CE}}{A^{\rm CE}-1}V_A^{\rm CE} - I_A^{\rm CE} \tag{27}$$

where $A^{\rm CB}$ and $C^{\rm CB}$ denote the $ABCD$ -parameters of the two-port device of the CB HBT. Using the definitions of (11)–(13), the CB noise parameters are obtained after some simple calculations as

$$R_n^{\rm CB} = \frac{R_n^{\rm CE}}{\left|A^{\rm CE}-1\right|^2} \tag{28}$$

$$G_n^{\rm CB} = \left|\frac{C^{\rm CE}}{A^{\rm CE}-1}\right|^2 R_n^{\rm CE} + G_n^{\rm CE} - 2{\rm Re}\left[\frac{C^{\rm CE}}{A^{\rm CE}-1}R_n^{\rm CE}Y_{\rm cor}^{\rm CE^*}\right] \tag{29}$$

$$Y_{\rm cor}^{\rm CB} = C^{\rm CE} - \left(A^{\rm CE}-1\right)Y_{\rm cor}^{\rm CE} \tag{30}$$

where $R_n^{\rm CE}$, $G_n^{\rm CE}$, $Y_{\rm cor}^{\rm CE}$ and $R_n^{\rm CB}$, $G_n^{\rm CB}$, $Y_{\rm cor}^{\rm CB}$ are the noise resistance, noise conductance, and correlation admittance of the CE and the CB configurations, respectively.

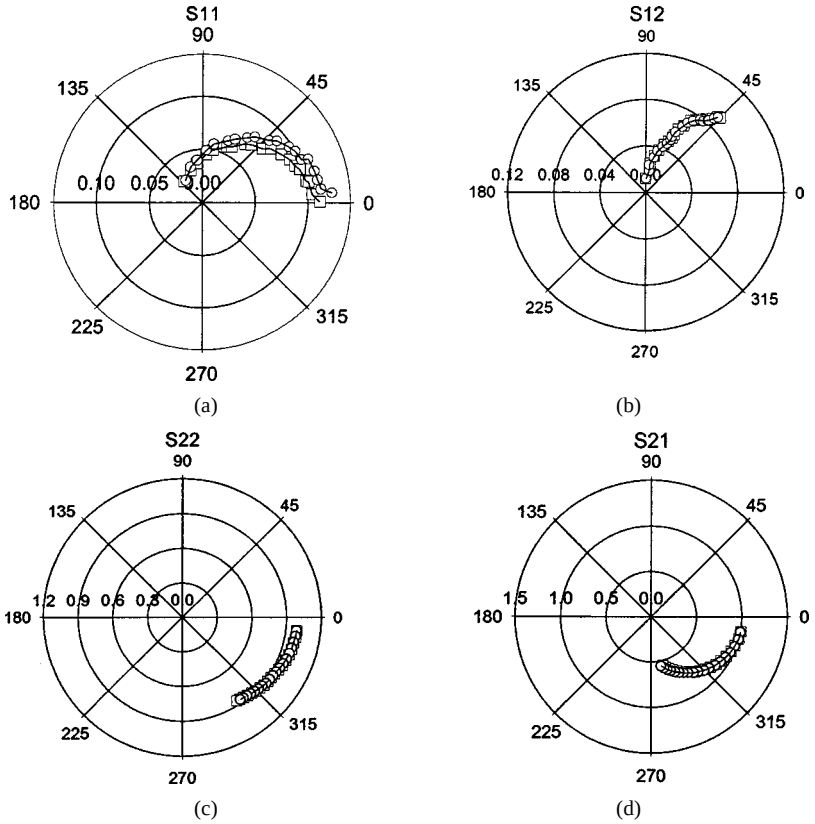

Fig. 3. Measured (□) and calculated (∘) CB S-parameters versus frequency at $V_{\rm CB} = 0.84$ V or $V_{\rm CE} = 1.5$ V and $I_C = 3.9$ mA.

III. Experimental Results

To verify the accuracy of the above noise transformation expressions, InP/InGaAs DHBTs in the CE and CB mode with an emitter area of 5×20 μm^2 were used in this study. Details of the device structure and performance were described in [10]. These CE devices showed an average extrinsic peak current gain of 180. The ideality factors of the collector and base currents were ∼1.1 and ∼1.2, respectively. The devices possess very low leakage current with a high CE breakdown voltage $(\mathrm{BV_{CEO}} > 9$ V). The CE devices have a typical current gain cutoff frequency (f_T) of 61 GHz and maximum oscillation frequency $(f_{\max})$ of 38 GHz. The $5 \times, 20$ μm^2 CB devices have a typical maximum oscillation frequency $(f_{\max})$ of 72 GHz.

The microwave noise parameters were measured from 2 to 20 GHz. The measurement system consisted of an ATN-NP5 wafer probe test set, HP8970C noise-figure test set, HP8970B noise-figure meter, and HP8510C network analyzer, and the signal source for the noise figure test set is shared with HP8510C. The minimum noise figure, noise resistance, and the optimal source impedance ($\mathrm{NF_{MIN}}$, R_N, $G_{\rm OPT}$, and $B_{\rm OPT}$) were extracted from the measured noise figure and S-parameters at a particular dc bias for these devices in the CE and CB configuration. Fig. 3 shows the comparison of the measured and calculated S-parameters of the CB configurations using (5)–(8) and S–Z transformations based on the CE small-signal parameters at $V_{\rm CB} = 0.84$ V or $V_{\rm CE} = 1.5$ V and $I_C = 3.9$ mA. Fig. 4 shows the comparison of the measured and calculated noise figure of the CB configuration using (15)–(17), (28)–(30) and CE noise figure at the same bias conditions. Good agreement between the measured and calculated S-parameter and minimum noise figure from 2 to 20 GHz were obtained. To further illustrate the effectiveness and accuracy of this approach, we also compared the measured $R_n^{\rm CB}$ and calculated $R_n^{\rm CB}$ from the measured $R_n^{\rm CE}$ at the same bias conditions. As shown in Fig. 5, good agreement is observed between the measured and calculated results despite the fact that the equivalent noise resistance is a difficult parameter to obtain because of the uncertainty in the S-parameter measurement. Figs. 6 and 7 show the measured real part $\left(G_{\rm opt}^{\rm CB}\right)$ and imaginary part $\left(B_{\rm opt}^{\rm CB}\right)$ of the optimum input admittance and the calculated $G_{\rm opt}^{\rm CB}$ and $B_{\rm opt}^{\rm CB}$ from the measured $G_{\rm opt}^{\rm CE}$ and $B_{\rm opt}^{\rm CE}$ at the same bias conditions. Although good agreement between the calculated and measured real part of the optimum input admittance was obtained, the errors between the measured and calculated real part increase with increasing frequency. This possible reason is that the measured errors are caused due to very small values of the imaginary part of the optimum input admittance.

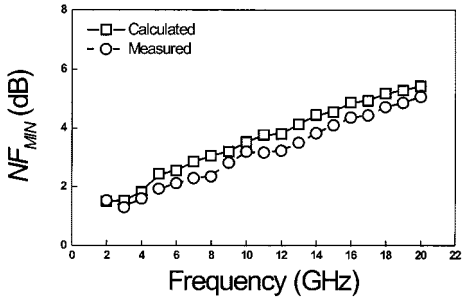

Fig. 4. Measured (□) and calculated (∘) CB noise figure versus frequency.

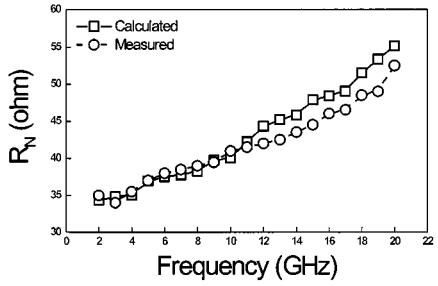

Fig. 5. Measured (□) and calculated (○) CB noise resistance versus frequency.

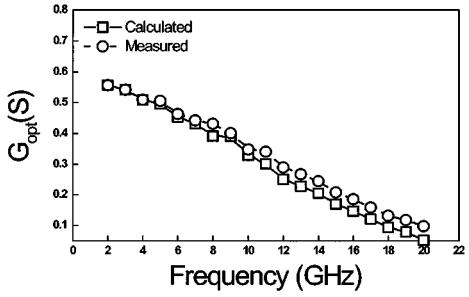

Fig. 6. Measured (□) and calculated (○) CB real part of the optimum input admittance versus frequency.

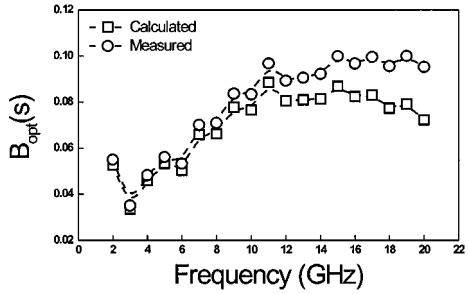

Fig. 7. Measured (□) and calculated (○) CB imaginary part of the optimum input admittance versus frequency.

IV. Summary

A set of formulas for quick noise parameter transformations based on the $ABCD$ representation for the CE and CB configurations has been presented. The simplified transformations of the Z-parameters between the CE and CB configurations have also been obtained. The measured microwave noise performances of an InP-based DHBT for the CB and CE configurations have been demonstrated to confirm these transformation. At the frequency range of 2–20 GHz, good agreements between the measured and calculated results of noise and S-parameters were obtained. This shows that the new approach for fast noise and Z-parameters transformations can be used for the application of the low noise and broad-band amplifier design. We believe that this approach also can be used for noise and S-parameter transformations between CB and CE configurations of other bipolar transistors. Therefore, a low-noise amplifier (LNA) can be built with any of the CE or CB configurations or combination thereof.

Acknowledgment

The authors wish to thank Prof. K. Radhakrishnan, Prof. S. F. Yoon, H. Q. Zheng, C. Y. Chen, H. Yang, and E. Yong, all of the Microelectronics Center, School of Electrical and Electronics Engineering, Nanyang Technological University, Singapore, for their helpful discussions and support.

References

[1] A. van der Ziel, *Noise in Solid State Devices and Circuits*. New York: Wiley, 1996.

[2] P. J. Fish, *Electronic Noise and Low Noise Design*. New York: McGraw-Hill, 1994.

[3] K. W. Kobayashi and A. K. Oki, "A low-noise baseband 5-GHz direct-coupled HBT amplifier with common-base active input match," *IEEE Microwave Guided Wave Lett.*, vol. 4, pp. 373–375, Nov. 1994.

[4] J. Martinez-Castillo and J. Silva-Martinez, "Transimpedance amplifiers for optical fiber systems based on common-base transistors," in *Proc. IEEE Int. Circuits Syst. Symp.*, vol. 6, 1999, pp. 85–88.

[5] J. B. Hagen, "Noise parameter transformations for three-terminal amplifiers," *IEEE Trans. Microwave Theory Tech.*, vol. 38, pp. 319–321, Mar. 1990.

[6] H. Hartman and M. J. O. Strutt, "Changes of the four noise parameters due to general changes of linear two-port circuits," *IEEE Trans. Electron Devices*, vol. ED-20, pp. 874–877, Oct. 1973.

[7] D. R. Pehlke and D. Pavlidis, "Evaluation of the factors determining HBT high-frequency performance by direct analysis of S-parameter data," *IEEE Trans. Microwave Theory Tech.*, vol. 40, pp. 2367–2373, Dec. 1992.

[8] B. Li and S. Prasad, "Basic expressions and approximations in small-signal parameter extraction for HBT's," *IEEE Trans. Microwave Theory Tech.*, vol. 47, pp. 534–539, May 1999.

[9] G. D. Vendlin, A. M. Pavio, and U. L. Rohde, *Microwave Circuit Design Using Linear and Nonlinear Techniques*. New York: Wiley, 1990.

[10] H. Wang, G. I. Ng, H. Zheng, Y. Z. Xiong, L. H. Chua, K. Yuan, K. Radhakrishnan, and S. F. Yoon, "Demonstration of aluminum-free metamorphic InP/$In_{0.53}Ga_{0.47}As$/InP double heterojunction bipolar transistors on GaAs substrates," *IEEE Electron Device Lett.*, vol. 21, no. 9, pp. 379–381, Sept. 2000.

[11] W. Dahlke, "Transformationsregeln fur rauschende vierpole," in *Arch. Elektr. Ubertragung*, 1955, vol. 9, pp. 391–401.

[12] P. Stangerup, "Electronic noise calculation by computer," Danish Res. Centre Appl. Electron., Hørsholm, Denmark, Tech. Rep. ECR-58, Feb. 1976.

Yong Zhong Xiong (M'98) received the B.S. and M.S. degrees in communication and electronic systems from the Nanjing University of Science and Technology (NUST), Nanjing, China, in 1986 and 1990, respectively, and is currently working toward the Ph.D. degree in electrical and electronic engineering at the Nanyang Technological University (NTU), Singapore.

From 1986 to 1992, he was an Engineer with NUST, where he was involved with microwave systems and circuit design. In 1992, he became a Lecturer in the Department of Electronic Engineering, NUST. From 1995 to 1997, he was with the RF and Radios Department, CEI Technologies Pte. Ltd., Singapore. As a Senior Engineer, he was also affiliated with the Centre for Wireless Communications, National University of Singapore, in 1996, where he was involved with the RFIT Project. Until the end of 1997, he was with the Microelectronics Centre, Nanyang Technological University (NTU), where he was a Research Associate. Since September 2001, he has been with the Institute of Microelectronics (IME), Singapore. His major areas of research include microwave device modeling, characterization, and monolithic microwave integrated circuit (MMIC) design.

Geok-Ing Ng (S'84–M'85–SM'00) received the B.S., M.S., and Ph.D. degrees in electrical engineering from The University of Michigan at Ann Arbor, in 1984, 1986, and 1990, respectively.

From 1991 to 1993, he was a Research Fellow at the Centre for Space Terahertz Technology, The University of Michigan at Ann Arbor, where he was involved with microwave/millimeter-wave semiconductor devices and MMICs. In 1993, he joined TRW Inc., Space Park, CA, where he was a Senior Member of Technical Staff engaging in research and development of GaAs and InP-based high electron-mobility transistors (HEMTs) for high-frequency low-noise and power MMIC applications. In 1995, he joined the Nanyang Technological University (NTU), Singapore, as a Lecturer with the School of Electrical and Electronic Engineering. He is currently an Associate Professor with NTU. In 1996, he became a Program Manager for the research and development projects on III–V RF devices and MMICs at the Microelectronics Centre, NTU. His current research interests include device physics, fabrication and characterization of microwave devices with different III–V material systems for low-noise, power, and MMIC applications.

Dr. Ng is a senior member of Tau Beta Pi and Eta Kappa Nu. He was the recipient of the 1990 European Microwave Prize for his work on InP-based heterostructure monolithic amplifiers.

Hong Wang (S'98–A'00–M'01) received the B.Eng. degree from Zhejiang University, Zhejiang, China, in 1988, the M.Eng. degree from the Nanyang Technological University (NTU), Singapore, in 1998, and is currently working toward the Ph.D. degree at NTU.

From 1988 to 1994, he was with the Institute of Semiconductors, Chinese Academy of Sciences, where he developed InP-based opto-electronic integrated circuits (OEICs). From 1994 to 1995, he was a Royal Research Fellow with British Telecommunications Laboratories, Ipswich, U.K., where he was involved with the development of 0.25-μm InP-based HFETs using E-beam lithography. Since 1996, he has been with the Microelectronics Centre, NTU, where he is currently a Research Associate. He has authored or co-authored over 40 technical papers. His current research interests are InP- and GaAs-based compound semiconductor device physics, fabrication technology, and characterization.

Chee Leong Tan (S'02) received the Electrical Engineering degree from the National University of Singapore, Singapore, in 1996.

Since 1996, he has been an Engineer with the Defence Science Organization National Laboratories, Singapore. His research interests are III–V compound semiconductor devices and circuits.

J. S. Fu (S'81–M'83–SM'92) received the Ph.D. degree in electrical engineering from Cornell University, Ithaca, NY, in 1983.

He possesses numerous years of professional experience with industries, institutions, and universities. In 1990, he joined the School of Electrical and Electron Engineering, Nanyang Technological University (NTU), Singapore, where he is currently an Associate Professor. He has authored or co-authored over 130 technical papers. His research interests are in microwave and millimeter-wave planar structure analysis, computer-aided design (CAD) modeling, circuit design, measurement, and characterization, and its application to personal communications and radar systems.